



Supplement of

Equilibrium absorptive partitioning theory between multiple aerosol particle modes

Matthew Crooks et al.

Correspondence to: Matthew Crooks (matthew.crooks@manchester.ac.uk)

The copyright of individual parts of the supplement might differ from the CC-BY 3.0 licence.

1 S1: Convergence of the dynamic model with mono-disperse modes

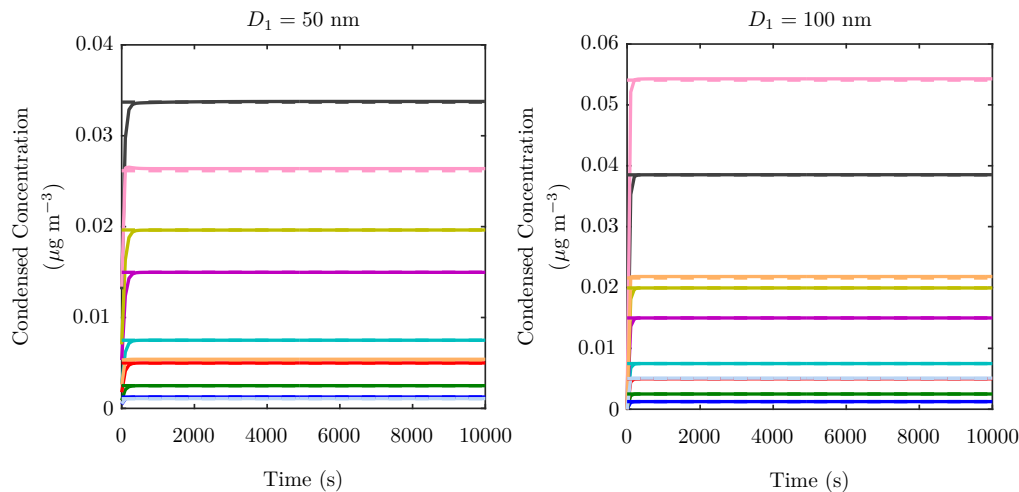


Figure 1. Time evolution of the total condensed concentrations of organics in each volatility bin in two runs of the dynamic model (solid lines). Each colour represents a different volatility bin and the solution from the partitioning theory is shown by the dashed lines. The left plot shows the condensed concentrations when the smaller mode has a diameter of 50 nm and in the right plot the smaller mode has a diameter of 100 nm. The median diameter of the second mode was 125 nm and the number concentrations of the first and second modes were 1000 cm^{-3} and 50 cm^{-3} , respectively. The relative humidity was 50% and the SVOC concentrations are given in Table 1.

We describe, here, the methodology that is used to ensure that the dynamic model has converged when comparing the equilibrium from the dynamic model against the equilibrium absorptive partitioning theory. The two solutions are compared against each other in the main paper.

5 For the results in the main paper, we initiate the dynamic model from a perturbed equilibrium state that places some of the SVOCs in the condensed phase on larger particles. This speeds up the equilibration of the dynamic model in order to obtain a well converged equilibrium solution. This is not intended to be atmospherically relevant. For comparisons between the dynamic model and the equilibrium absorptive partitioning solution under atmospherically relevant timescales the reader is
10 directed towards Section S3.

The initial condensed mass is motivated by knowledge that the equilibrium absorptive partitioning solution places the majority of the condensed mass at equilibrium on the larger mode (given the number concentrations used in this paper) and so starting the main simulations with a large portion of the SVOCs in the condensed phase on larger particles allows the simulation to start closer to the
15 equilibrium solution. In order to avoid biasing the dynamic model by actually using the equilibrium absorptive partitioning theory as an initial condition, we derive the initial condensed masses by running the dynamic model for between ten and a few hundred seconds. We initiate it with all the SVOCs in the condensed phase and allow condensation of the organic compounds onto the larger particles only. The dynamic model is then reinitialised with these calculated condensed masses on
20 the larger mode as an initial condition and the remaining SVOCs occurring in the vapour phase. The subsequent time evolution of the condensed concentrations across all particles are then calculated.

The dynamic model was run twice with the parameters given in Tables 2 and 3 at the temperature and pressure given in Table 4, together with a relative humidity of 50%. The SVOC concentrations are stated in Table 1. The first mode had a diameter of 50 nm in the first simulation and 100 nm in
25 the second. To calculate the initial condensed mass, the larger particles were given initial periods of 300 seconds of simulation time in the first model run. In the second, the diameter of the smaller mode is sufficiently similar to the large mode that no initial equilibration period was required. The

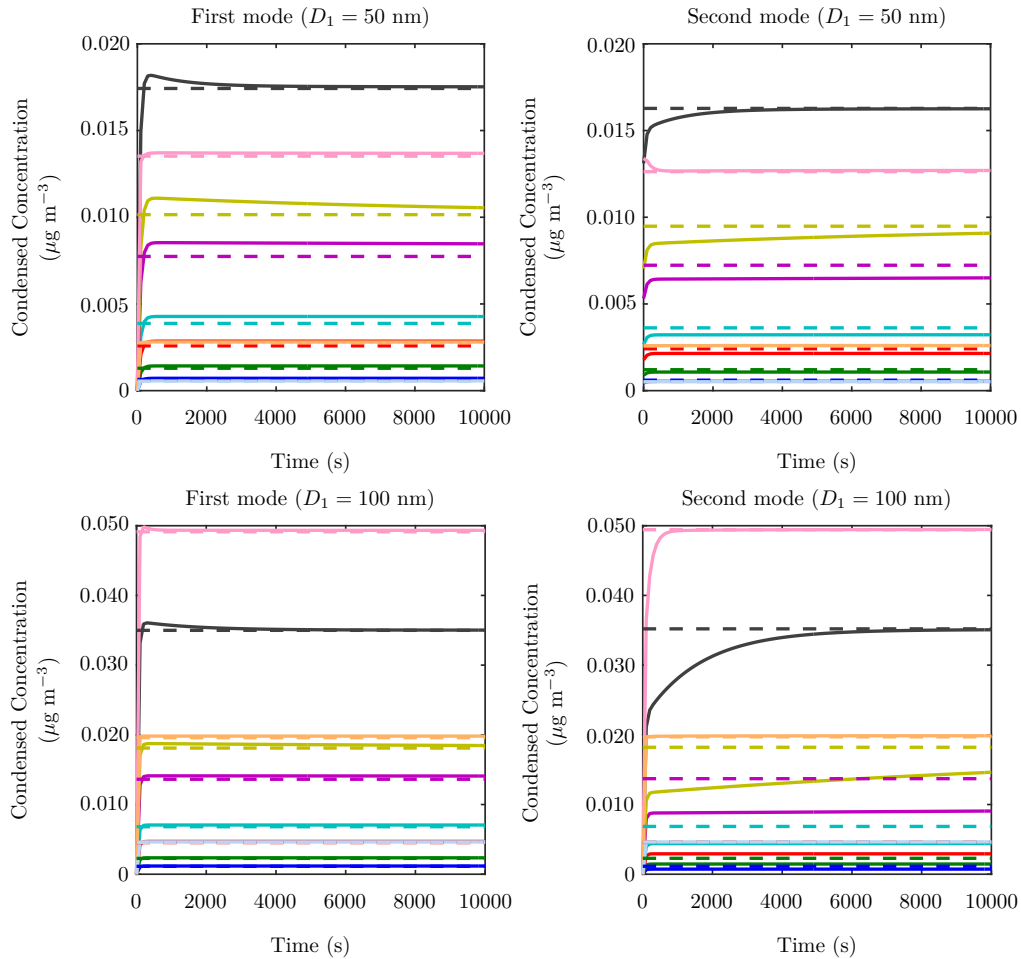


Figure 2. Time evolution of the condensed concentrations of organics from Figure 1 split across the two individual modes. The top two plots shown the individual condensed concentrations on each of the modes when the smaller mode has a diameter of 50 nm and the lower two plots show the results when the smaller mode has a diameter of 100 nm. The left plots show the condensed concentration on the smaller mode and the right plots are for the large of the two modes used in the simulations.

subsequent time evolution of the total condensed masses across both modes are shown by the solid lines in Figure 1 for a relative humidity of 50%. Bulk equilibrium is reached by about 1000 seconds

30 with the individual modes reaching equilibrium by approximately 10000 seconds, as seen in Figure 2. The dynamic model converges on a value which is in excellent agreement with the partitioning theory shown by the dashed lines. The dynamic solution at 10000s is used in Section 6.1 of the main paper as an approximation to the equilibrium from the dynamic model.

35 The additional plots in the main paper in Figure 9 with a smaller mode with median diameters of 25 nm and 75 nm were initiated after the large particles had had 1500 s and 100 s to equilibrate, respectively. The plots in Figure 10 were given initial equilibration periods of 800 s, 800 s, 600 s and 400 s for the 100 cm^{-3} , 250 cm^{-3} , 500 cm^{-3} and 750 cm^{-3} simulations, respectively.

Table 1. Volatility distribution of SVOCs.

$\log \mathcal{C}^*$	-6	-5	-4	-3	-2	-1	0	1	2	3
Concentration ($\mu\text{g m}^{-3}$)	0.00125	0.0025	0.005	0.0775	0.015	0.02	0.04	0.075	0.105	0.2

Table 2. Material parameters used in the dynamic model simulations. The SVOC concentrations are stated in Table 1.

variable	ρ_i^o (kg m^{-3})	ρ_j (kg m^{-3})	M_j (kg mol^{-1})	M_i^o (kg mol^{-1})	ν_i^o	ν_j
value	1770	1500	0.132	0.2	3	1

Table 3. Range of values assigned to the number concentration, N_i , and involatile particle diameter, D_i , used in the dynamic model simulations.

variable	N_i (cm^{-3})	D_i (nm)
mode 1	1000	50, 100
mode 2	50	125

Table 4. Temperature and pressure used in the dynamic models

parameter	P (Pa)	T (K)
Initial value	95000	293.15

2 S2: Convergence of the dynamic model with lognormal distributed particle modes

Extending multiple mode equilibrium absorptive partitioning theory to the case when each mode is represented by a lognormal size distribution of particles introduces some errors. These occur due to each size of particle within a lognormal mode having a different equilibrium vapour pressure over its surface. By modelling all particles within a mode as a single entity, the Kelvin term and the value of C_T must be replaced by effective values and will not agree with the analogous values of individual particles. The purpose of Section 6.2 in the main paper is to study the errors introduced by using lognormal size distributions for each mode in the equilibrium absorptive partitioning theory. In order to do this, we wish to isolate the errors due to the convergence of the dynamic model to equilibrium from the errors resulting from using a size distribution of particles in each mode.

We employ the same method as described in Section 1 in which we place some of the organic compounds on the larger particles at the start of the simulations that generate the results in the main paper. The amount of condensed mass on the larger particles at the start of the simulations is calculated by running the dynamic model with just the large particles for an initial period, starting with all of the SVOCs in the vapour phase. Again, this is just to speed up convergence towards equilibrium and reduce errors in stopping the dynamic model at a finite time. In the case of lognormal modes, however, this process is a little different as a particle size bin may contain particles from both the smaller and the larger modes and cannot distinguish between the two. To overcome this, rather than simply condensing mass onto the larger mode when deriving the initial conditions, we condense mass on to any size bin in which more than 1% of its particles are from the larger mode.

In this section we show that this method does lead to convergence both of the bulk condensed mass and the condensed mass on each individual mode. Comparisons between the equilibrium of the dynamic model and the equilibrium absorptive partitioning theory solution are compared in the main paper.

The dynamic model was run with the parameters given in Table 5 together with the material properties from Table 2 and temperature and pressure from Table 4. The SVOC concentrations are stated in Table 1. We used 140 size bins in total with each containing the same number of aerosol particles. The larger size bins were given an initial period of 1500 seconds of simulation time before the smaller particles were added. Again, this speeds up the convergence of the dynamic model towards equilibrium to allow comparison between its limiting behaviour and our equilibrium partitioning theory applied to lognormal modes. The subsequent time evolution of the condensed concentrations are shown by the solid lines in Figure 3 for a relative humidity of 0% and 90%. Bulk equilibrium is reached by about 2000 seconds and the dynamic model converges on a value which is in good agreement with the equilibrium absorptive partitioning theory shown by the dashed lines.

Table 5. Size distribution parameter values used in the dynamic model simulations

variable	N (cm^{-3})	D_m (nm)	$\ln \sigma$
mode 1	200	25	0.5
mode 2	50	125	0.1

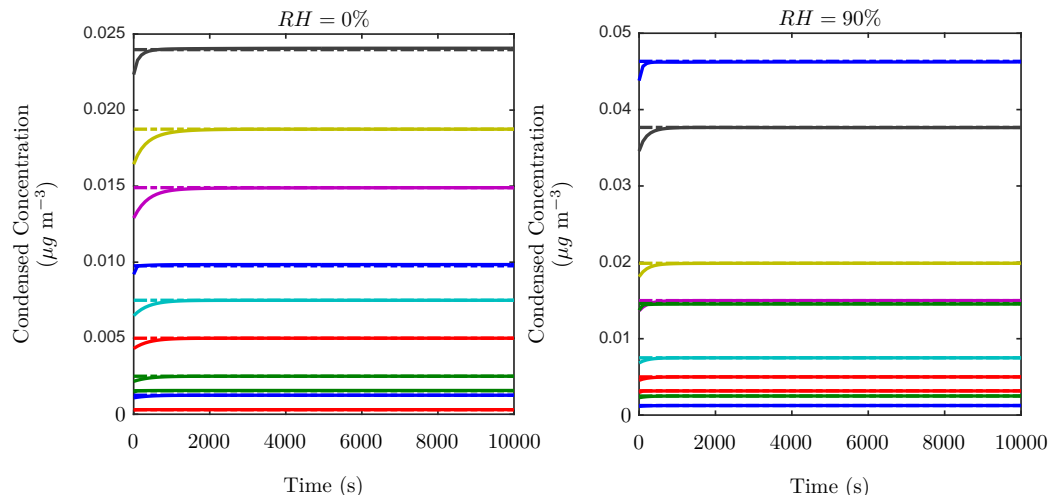


Figure 3. Time evolution of the total condensed concentrations of each organic in the dynamic model (solid lines) for $RH = 0\%$ (left) and $RH = 90\%$ (right). The size distributions are defined by the parameters in Table 5 and the relative humidity is stated above each plot. SVOC concentrations are given in Table 1.

Figure 4 shows how the condensed concentrations from Figure 3 are split between the two individual modes with the left plots showing the smaller mode and right plots showing the larger mode. Simulations were run for 10000 seconds for $RH = 0\%$ and $RH = 90\%$ and although the organic 75 shown by the yellow line has not completely reached equilibrium on the first mode it is assumed to be sufficiently close. Again, the condensed masses calculated by the dynamic model at 10000s are used in the main paper.

3 S3: Application to large scale models

It is shown in the main paper that equilibrium absorptive partitioning theory agrees well with the 80 equilibrium from the dynamic model. This is especially true for mono-disperse aerosol modes but there is also excellent agreement when each mode is represented by a lognormal size distribution with median diameter above 50 nm. For those comparisons we calculated a solution close to the

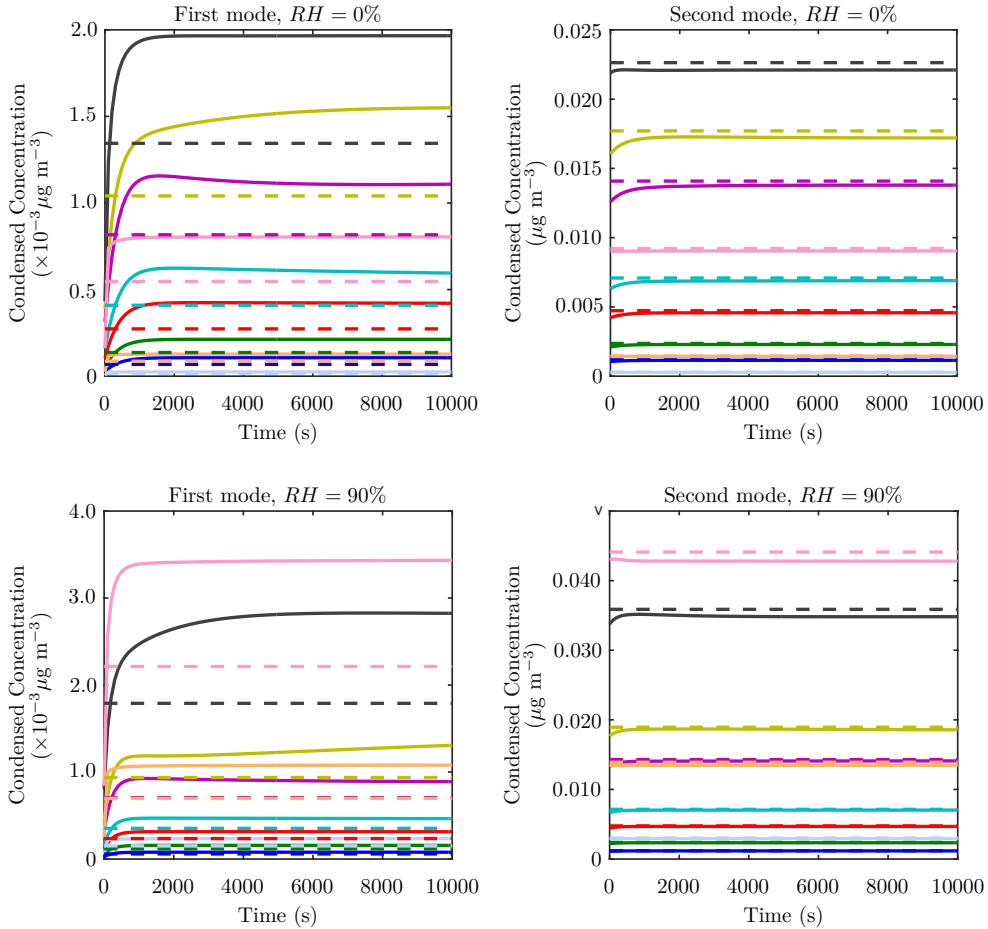


Figure 4. Time evolution of the individual condensed concentrations on each of the modes in the dynamic model for $R_H = 0\%$ (top) and $R_H = 90\%$ (bottom). The smaller mode is shown on the left and the larger on the right.

equilibrium in the dynamic model that would be obtained if it were left running for an infinite length of time. In large-scale models much shorter finite time-scales are used and we now investigate the
85 magnitude of the errors that would be introduced as a result of approximating the dynamic model with equilibrium absorptive partitioning theory at these time-scales.

Two different scenarios have been simulated in which we compare equilibrium absorptive partitioning theory against the dynamic model while the SVOCs are still condensing dynamically. In the first case, we start the simulations with all SVOCs in the vapour phase and allow them to condense
90 on to all particles simultaneously while holding temperature, pressure and RH constant. This is designed to see how long it takes for the SVOCs to equilibrate after being emitted from an emissions source. The second scenario investigates the effect of small perturbations in temperature, pressure and RH. It is designed to investigate whether the SVOCs can return to equilibrium at the perturbed meteorological parameter values within one time-step of a large-scale model. In this case we start
95 from equilibrium, calculated using equilibrium absorptive partitioning theory, perturb the temperature, pressure and RH and calculate the condensed masses from the dynamic model after 15 minutes and 30 minutes. These are then compared against equilibrium absorptive partitioning theory calculated at the perturbed temperature, pressure and RH.

3.1 S3.1: Equilibration timescales near emissions sources

100 This section shows the results from the dynamic model for time periods of up to 3 days after the particles first interact with the semi-volatile vapours when the temperature, pressure and relative humidity are held constant. In these simulations we start with all of the SVOCs in the vapour phase and are designed to study the initial equilibration period directly after emission of both the non-volatile particles and the SVOC vapours. Estimates of the residence times of aerosol particles in
105 the atmosphere vary significantly with as long as 65 days being reported in one study (Marencio and Fontan, 1973). The majority of the literature, however, predicts residence times of 5 - 15 days (Paspastefanou, 2006; Ahmed et al., 2004; Balkanski et al., 1993) and so the 3 day time is chosen as this is well within the lifetime of aerosol particles in the atmosphere. Aerosol parameters are given in Table 2 and Table 5 along with temperature, pressure and relative humidity given in Table 4.
110 Figure 5 shows the time evolution of the condensed masses on the two lognormal modes from the dynamic model after times of 12 hours, 24 hours and 72 hours of condensation at constant temperature, pressure and RH. These are compared against the solution to equilibrium absorptive partitioning theory. The equilibrium plot is the same as the lower right plot in Figure 11 in the main paper and, as previously discussed, for some compounds the dynamic model solution is about 50%
115 higher than the equilibrium absorptive partitioning solution. Compared against the dynamic solution, the equilibrium absorptive partitioning theory performs less well on the smaller mode. Even by 12 hours, the lower 5 volatility bins are significantly higher in the dynamic solution than is calculated by equilibrium absorptive partitioning. This is because the lower C^* value means these compounds evaporate and condense more slowly than the higher volatility compounds. The additional condensed
120 mass in these volatility bins causes additional mass in the higher volatility bins to remain in the condensed phase on the smaller mode. By 72 hours the two solutions are in better agreement but there is still a large disparity in the lower 4 volatility bins.

125 Figure 6 shows the absolute value of the relative error of the total condensed mass of SVOCs across all volatility bins from equilibrium absorptive partitioning theory against the dynamic solution at times corresponding to the plots in Figure 5. At equilibrium the total errors in mass are about 35% with the majority of this mass coming from the higher volatility bins; shown by the more abundant purple shades. After 12 hours of dynamic condensation the errors are about 70% and are much more equally apportioned across all the volatility bins. About half of this error, however, is attributed to the use of a lognormal size distribution in the equilibrium partitioning theory. Even after three days
130 there is still over 60% errors in the partitioning theory solution.

135 In Section 6.2 it was found that using a lognormal mode with a median diameter of 50 nm rather than 25 nm gave much better agreement between the equilibrium absorptive partitioning theory and the dynamic model at equilibrium. The dynamic model additionally converges on equilibrium much quicker in the 50 nm case. Figure 7 shows the condensed mass from the dynamic model at a range of times after initiation and even after just 2 hours the solution from the dynamic model
140 is comparable to equilibrium absorptive partitioning theory with almost perfect agreement in the upper four volatility bins. By 24 hours the errors reduce even further and are restricted to the lower 5 volatility bins. Figure 8 shows the error bars in total condensed mass corresponding to Figure 7. At equilibrium the errors are less than 4% which is the lower limit of the errors obtainable using the current lognormal size distributions. After 2 hours of condensation the error in total condensed mass assuming equilibrium partitioning is only about 17% on the smaller mode and this decreases to 12% by 24 hours. In a global model, 2 hours may be modelled by only 4 time steps of 30 minutes and so using equilibrium absorptive partitioning theory gives a reasonably good approximation to the dynamic process of condensation within just a few time steps.

145 3.2 S3.2: Condensation during a single time-step

We now investigate how quickly the condensed masses of SVOCs equilibrate when the temperature, pressure and relative humidity are perturbed, assuming initial condensed masses are in equilibrium.

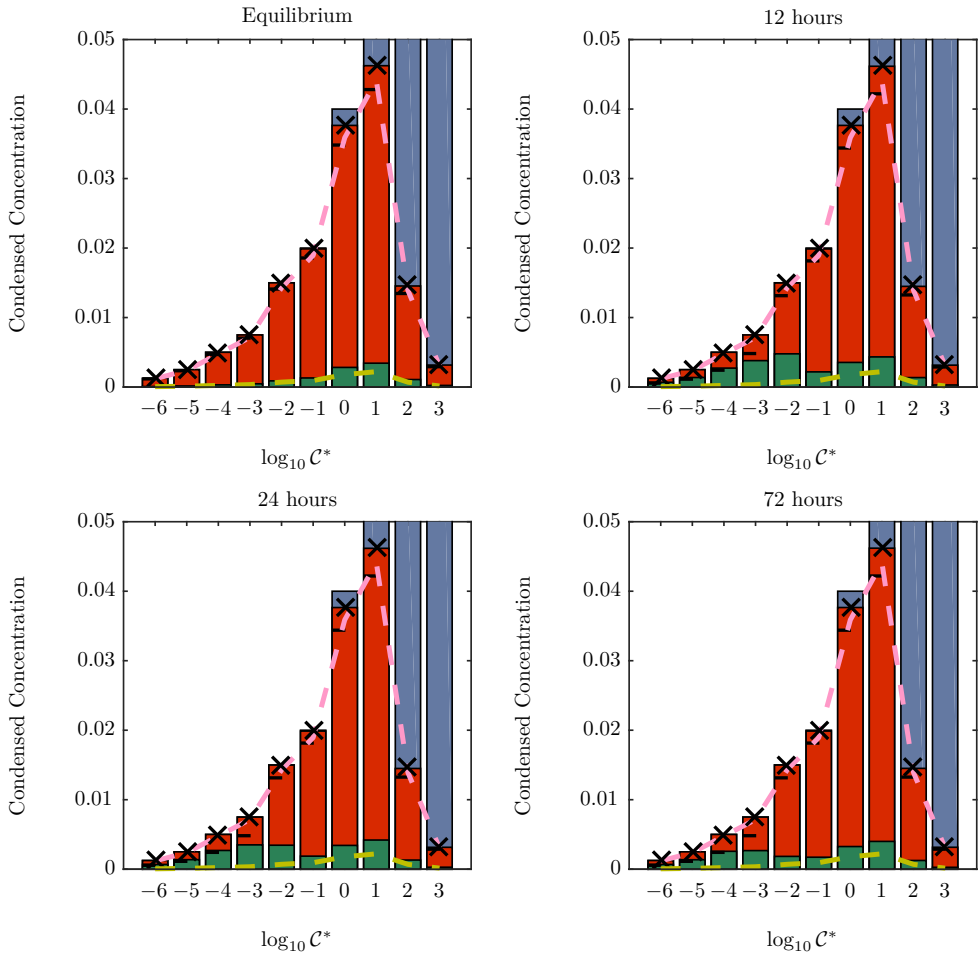


Figure 5. Comparison between condensed mass calculated using equilibrium partitioning theory against the dynamic condensation solution at a range of times. Aerosol size distribution parameters are given in Table 5 and the SVOC concentrations are given in Table 1. The temperature and pressure are stated in Table 4 and the relative humidity was 90%.

This section is designed to study whether equilibrium can still be assumed after meteorological parameter values change between time-steps in a large-scale model.

150 Initial condensed masses are calculated using equilibrium absorptive partitioning theory at the temperature and pressure values given in Table 4 and a relative humidity of 90% before adding perturbations of -2°K , -50 Pa and 5%, respectively. The dynamic model was then used to calculate the subsequent condensation. The dynamic model is evaluated at 15 minutes and 30 minutes and the condensed masses on the first and second modes are shown by the stacked green and red bars in Figures 9 and 10. Equilibrium absorptive partitioning theory was used to calculate the equilibrium condensed masses at the perturbed temperature, pressure and relative humidity and these are shown by the yellow and pink dashed lines. Initial condensed masses are shown by the dashed grey line. Figure 9 shows the results for the aerosol parameters given in Table 2 and Table 5 while Figure 10 shows the analogous results when the median diameter of the first mode is increased to 50nm.

155 The dashed grey line shows the initial total condensed mass and the tops of the red sections of the bars indicate the total condensed mass from the dynamic model. Perturbing the meteorological parameters has induced a significant increase in condensed mass and confirms that the re-equilibration at the perturbed meteorological parameters is not a trivial calculation.

160 The dashed grey line shows the initial total condensed mass and the tops of the red sections of the bars indicate the total condensed mass from the dynamic model. Perturbing the meteorological parameters has induced a significant increase in condensed mass and confirms that the re-equilibration at the perturbed meteorological parameters is not a trivial calculation.

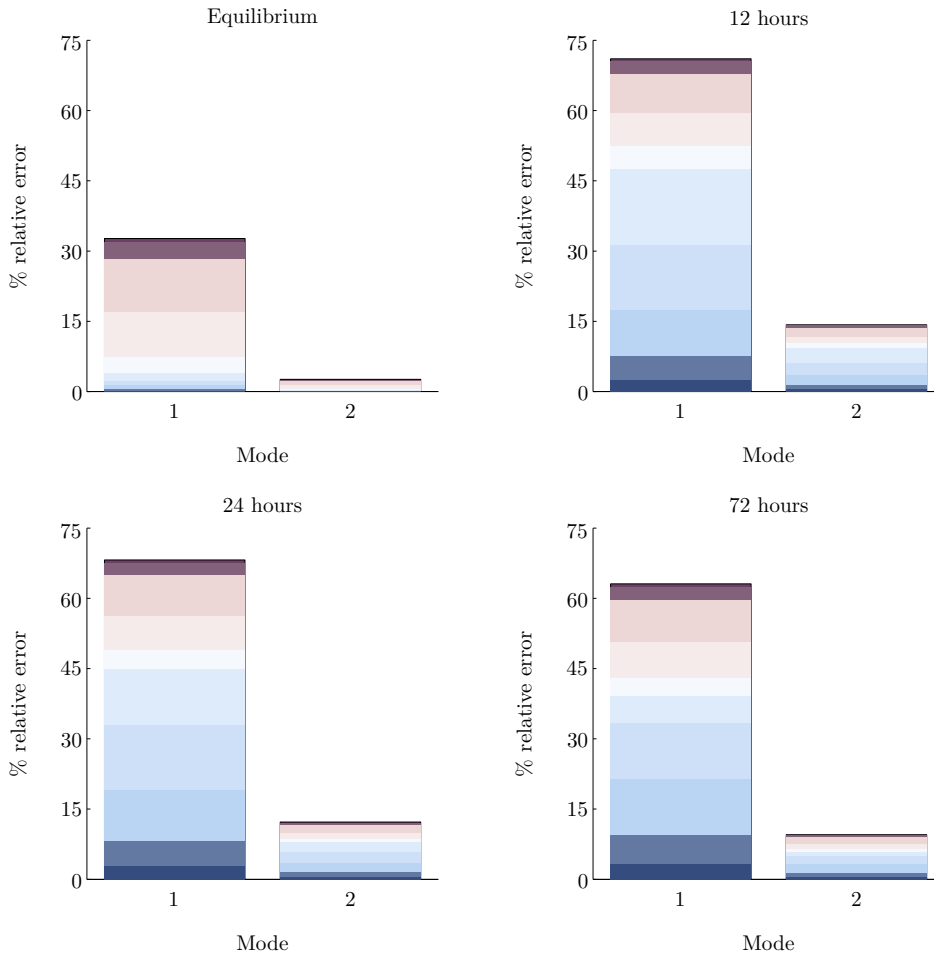


Figure 6. Relative error of the condensed mass from equilibrium partitioning theory onto 2 lognormal size distributions compared against the dynamic solution. Each subfigure corresponds to plots in Figure 5. The bars are subdivided to show the contribution from each volatility bin and are coloured with low C^* values in dark blue and high C^* values in dark purple.

In the case of Figure 9 there are some discrepancies between the condensed masses calculated using equilibrium absorptive partitioning theory and the dynamic model with the most notable on the smaller mode. This disagreement between the models, however, is most likely down to the errors in the equilibrium absorptive partitioning theory solution when applied to a lognormal mode with median diameter below 50 nm. The errors look broadly similar in magnitude to those seen in Figure 11 in the main paper and it is most likely that the dynamic model has converged in 15 minutes after perturbing the meteorological parameters but that this equilibrium does not agree with that calculated using equilibrium partitioning theory because of the Kelvin term, as discussed in Section 6.2 of the paper.

Figure 10 shows the results for a smaller mode with median diameter of 50 nm. In previous plots, it was found that for median diameters at or above 50 nm the dynamic model and the equilibrium absorptive partitioning theory agree well; this is further demonstrated in Figure 10. The equilibrium partitioning solution on the first and second modes (yellow and pink dashed lines) lie perfectly on top of the green bars and the horizontal black lines showing the analogous quantities from the dynamic model.

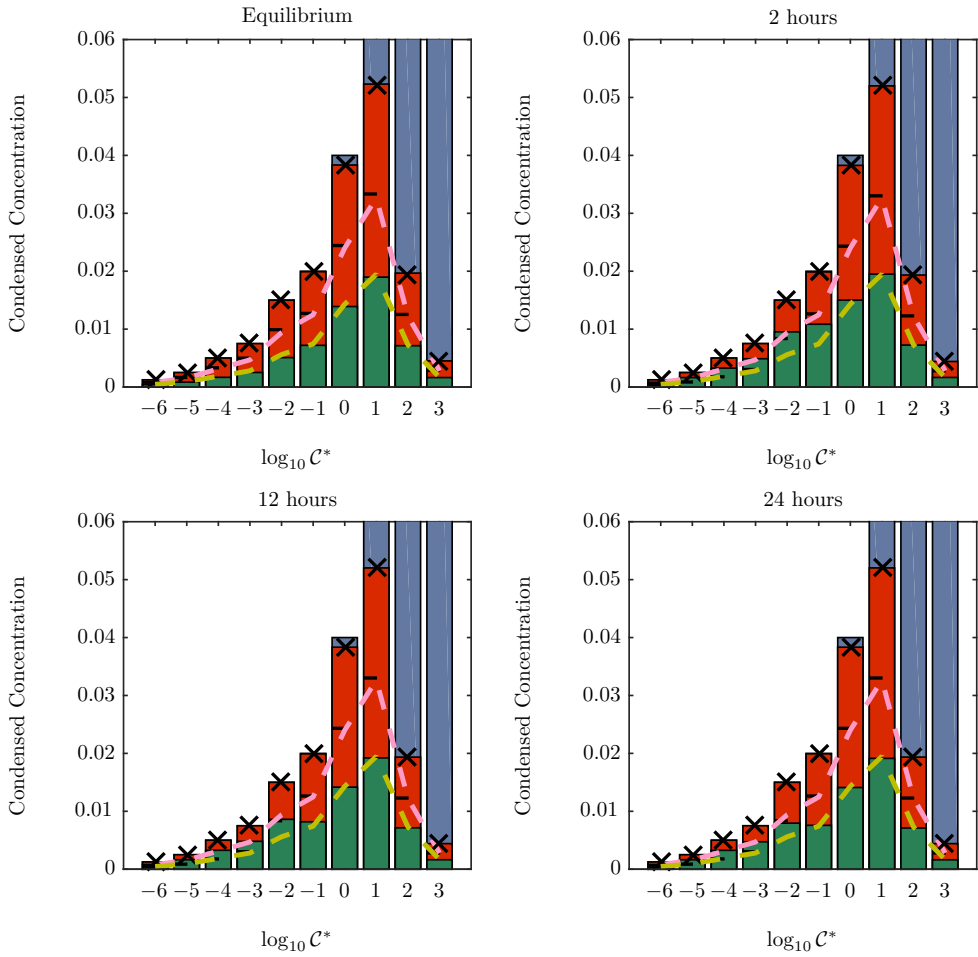


Figure 7. Same as Figure 5 but the smaller mode has a median diameter of 50 nm.

Little difference can be seen between the solution from the dynamic model after 15 minutes compared to 30 minutes in both Figures 9 and 10 allowing us to conclude that the condensed masses of SVOCs equilibrate in under 15 minutes after perturbing the meteorological parameters. The quick equilibration time is down to the fact that the additional condensed mass comes from the higher C^* volatility bins and these can evaporate and condense rapidly. Consequently, in large-scale models with time-steps of 15 minutes or more multiple mode equilibrium absorptive partitioning theory can be used to quickly and efficiently calculate the condensed mass of SVOCs during large-scale transport of aerosol. Using shorter time-steps does not mean that equilibrium absorptive partitioning theory cannot be used, we have simply not investigated shorter time frames for the dynamic condensation.

4 S4: Size Distribution

Calculating the change in size distribution as a result of condensing SVOCs is very much a dynamical process (Pandis et al., 1993; Wexler and Seinfeld, 1990; Zhang et al., 2012); not only are the organic compounds condensing onto each mode as a whole but they are also evaporating and condensing between the different sizes of particles within each mode. In the equilibrium absorptive partitioning theory calculations in Section 6.2 we assumed that the geometric standard deviation of the size

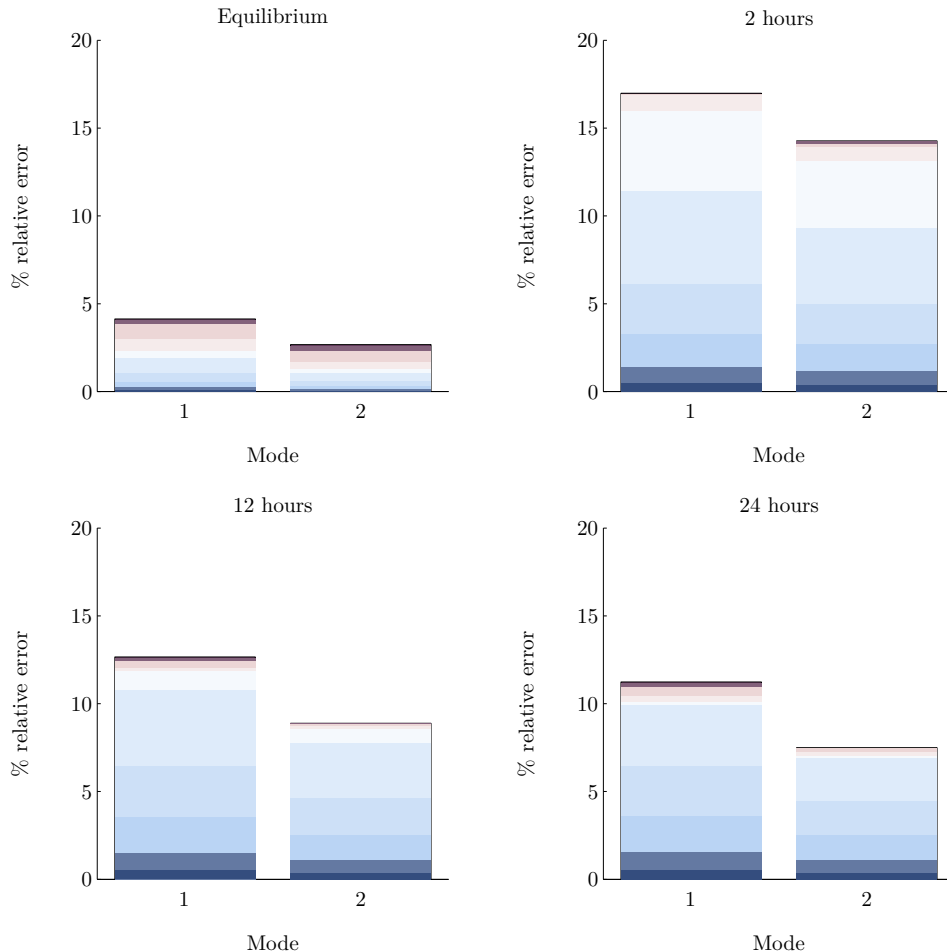


Figure 8. Same as Figure 6 but showing the errors in Figure 7 with a median diameter of the smaller mode of 50 nm.

195 distribution, $\ln \sigma$, remained unchanged by the additional condensed mass of SVOCs and water. This allowed the new median diameter of the wet aerosol particles to be calculated using conservation of mass. We analyse in this section whether this method results in an accurate approximation to the size distribution from the dynamic model under the condensation conditions investigated in Section S3.1.

200 Figures 11 and 12 show the size distributions from the dynamic model corresponding to Figures 5 and 7 against the size distribution calculated using equilibrium absorptive partitioning theory. Aerosol parameters used for Figure 11 are given in Table 2 and Table 5 along with temperature and pressure given in Table 4 and a relative humidity of 90%. Figure 12 show the same but the smaller mode has a median diameter of 50 nm.

205 Initial dry size distributions are shown by the solid grey lines. The crosses show the wet size distributions from the dynamic model and the solid blue lines correspond to the equilibrium absorptive partitioning theory. The dynamic model equilibrium plots in the top left of Figures 11 and 12 were evaluated after 1 million seconds of simulation time and are assumed to accurately represent equilibrium. The condensed masses of SVOCs are in excellent agreement for the 50 nm case (see Section S3.1) and so the top left plot of Figure 12 compares the size distribution from the dynamic model compared to the constant $\ln \sigma$ approximation without errors from the condensed masses of SVOCs. Assuming a constant $\ln \sigma$ can, therefore, accurately capture the wet size distribution at equilibrium.

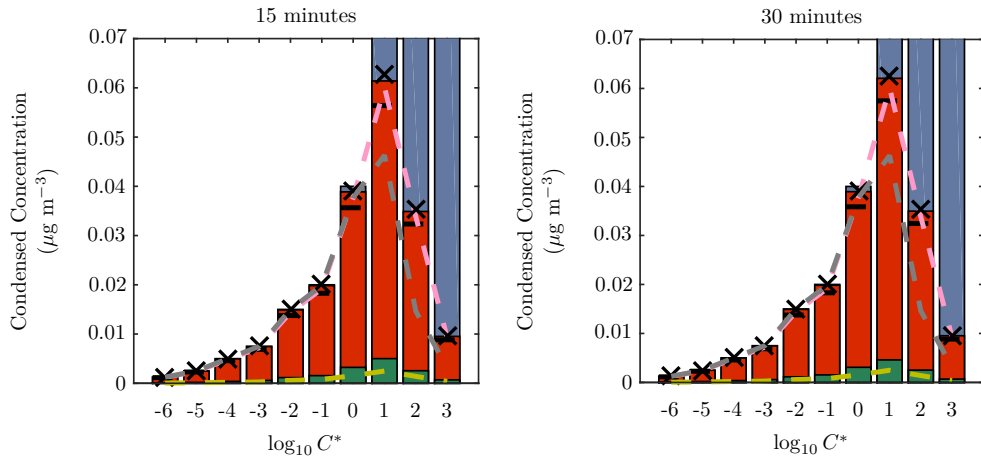


Figure 9. Comparison between condensed mass calculated using equilibrium partitioning theory against the dynamic condensation solution after perturbing temperature, pressure and relative humidity. The dashed lines show the solutions from equilibrium absorptive partitioning theory. The yellow and pink lines are the condensed mass on the first and second modes, respectively, at the perturbed temperature, pressure and RH while the grey dashed line shows the initial total condensed mass. The bars are coloured to show the solution from the dynamic model after condensation at the perturbed temperature, pressure and RH has occurred for 15 minutes (left) and 30 minutes (right). Aerosol parameter values are given in Table 2 and Table 5. SVOC concentrations are given in Table 1

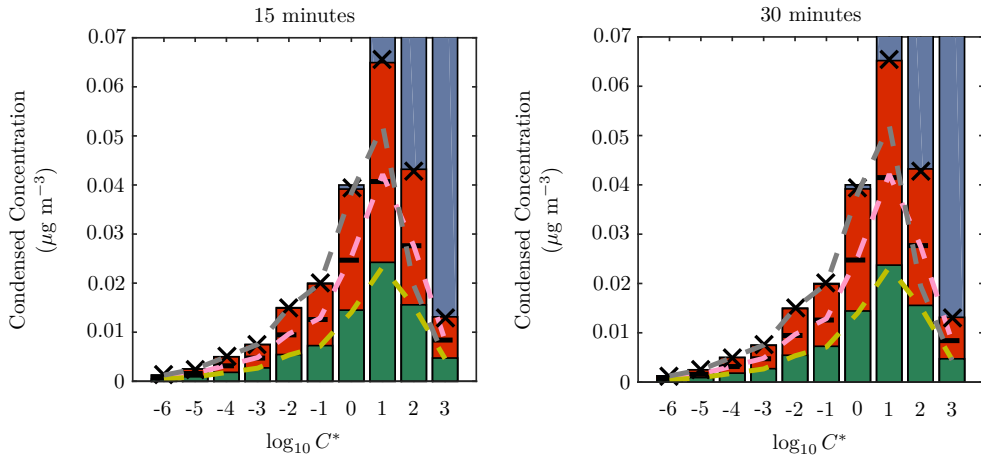


Figure 10. Same as Figure 9 but the first mode has a median diameter of 50nm

In the top left plot of Figure 11, the errors from the condensed masses of SVOCs from equilibrium absorptive partitioning theory for a mode with a median diameter of 25 nm result in a slight discrepancy in the size distribution. The errors, however, are only small and the size distribution of the larger mode is accurately captured.

The other plots in Figure 11 show the same size distribution from the equilibrium absorptive partitioning theory but the dynamic model is still evaporating and condensing SVOCs onto particles of different sizes. In all cases, the wet size distribution of the larger mode is accurately approximated with a constant geometric standard deviation. The smaller mode shows some significant disagreement, even after 72 hours. This is likely to be the result of the under prediction of condensed mass from equilibrium absorptive partitioning theory rather than the assumption of constant $\ln \sigma$.

The dynamic plots in Figure 12 show good agreement between the dynamic model and the equilibrium absorptive solution. After 2 hours of dynamic condensation there is some under prediction in particle sizes from the equilibrium partitioning theory but these are small and are mostly removed by the 12 hour plots. There is little difference between dynamic solution in the 12 hour, 24 hour and equilibrium plots and it can consequently be concluded that the size distribution in this case has reached equilibrium after a period of between 2 hour and 12 hours. The size distribution of wet aerosol particles can, therefore, be accurately approximated using equilibrium absorptive partitioning theory, together with the assumption that the geometric standard deviation is not affected by the condensing SVOCs.

225 In many situations, wet aerosol sizes are an important factor, such as in radiative forcing calculations, and equilibrium partitioning together with maintaining a constant geometric standard deviation could provide a quick method of accurately capturing the wet size distribution.

230

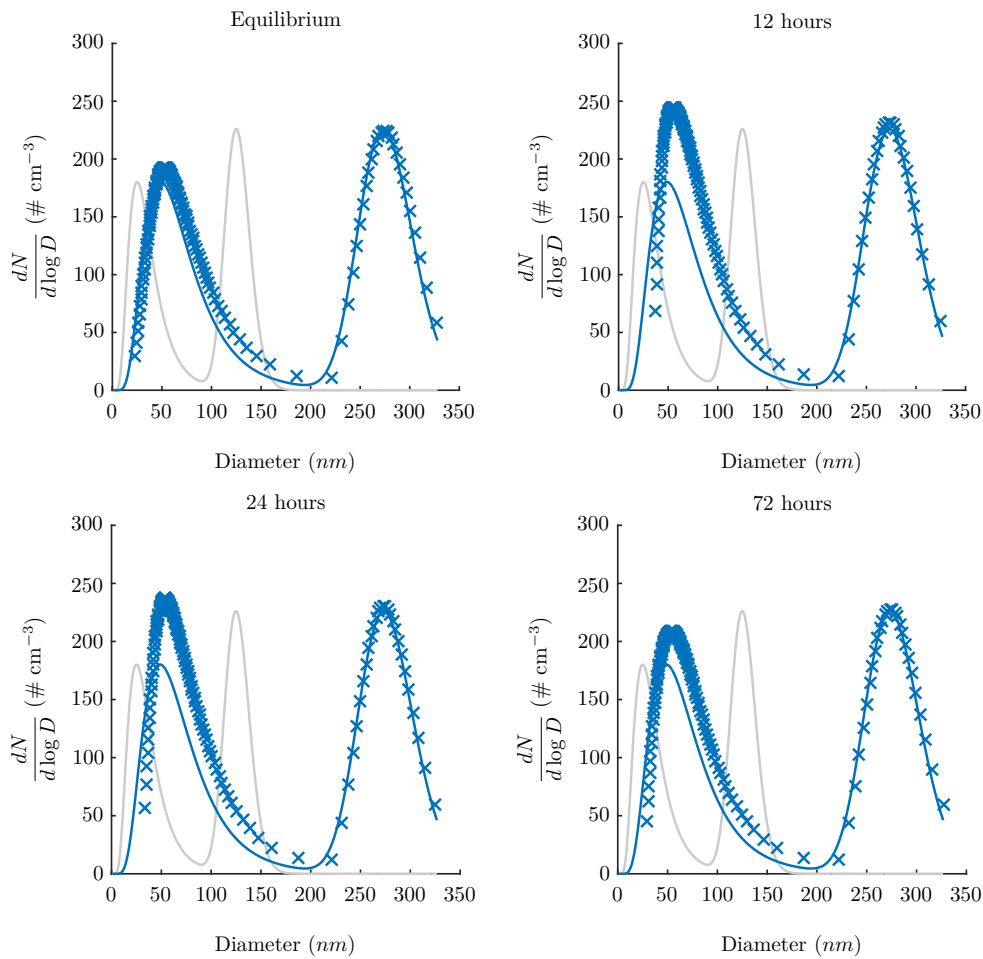


Figure 11. Time evolution of the size distribution. The grey line shows the initial size distribution of ammonium sulphate and the blue show the wet aerosol size distributions. The crosses are from the dynamic model, the solid lines are from equilibrium partitioning assuming constant geometric standard deviation. Total SVOC mass loading is $0.47 \mu\text{g m}^{-3}$.

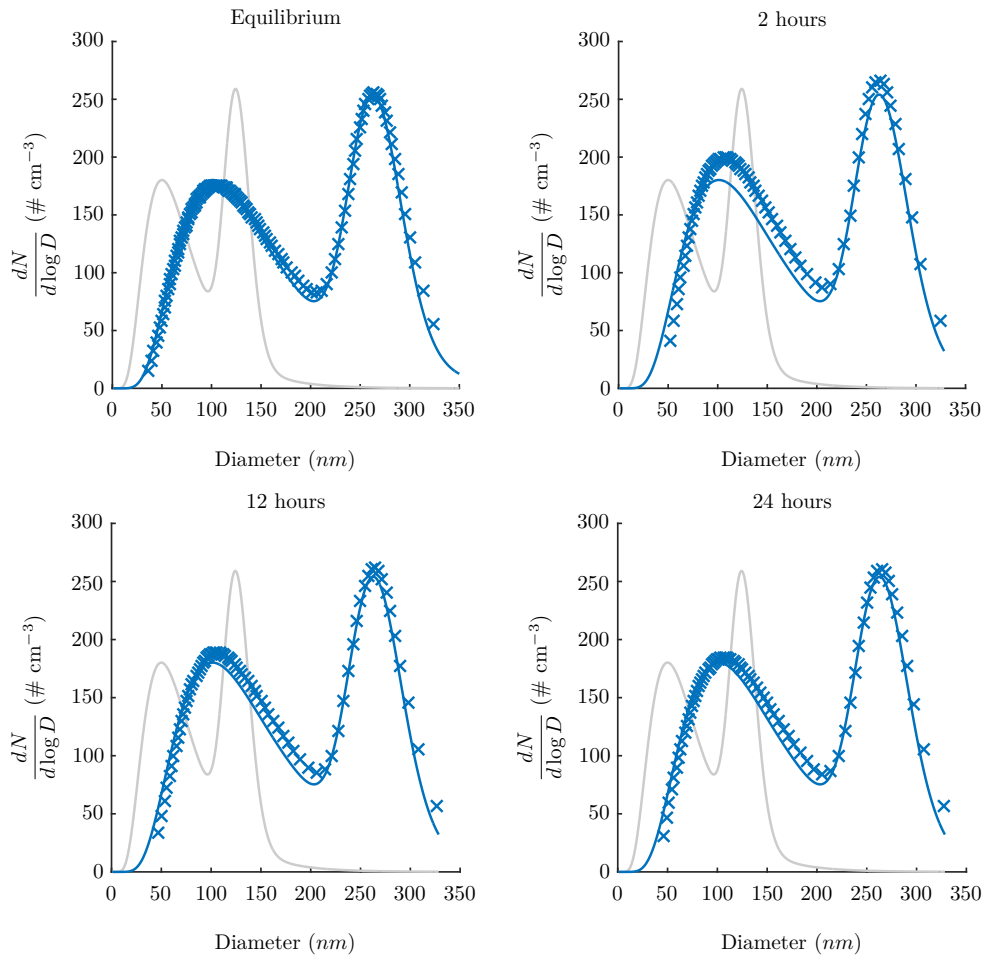


Figure 12. Same as Figure 11 with the first mode of median diameter 50 nm.

235 References

Ahmed, A., Mohamed, A., Ali, A., Barakat, A., Abd El-Hady, M., and El-Hussein, A.: Seasonal variations of aerosol residence time in the lower atmospheric boundary layer, *J. Environ. Radioact.*, 77, 275 – 283, 2004.

Balkanski, Y., Jacob, D., and Gardner, G.: Transport and residence times of tropospheric aerosols inferred from a global three-dimensional simulation of ^{210}Pb , *Journal of Geophysical Research*, 98, 20 573 – 20 586, 1993.

240 Marenco, A. and Fontan, J.: Sources of polonium 210 within the troposphere, *Tellus*, 25, 1973.

Pandis, S., Wexler, A., and Seinfeld, J.: Secondary organic aerosol formation and transport - II. Predicting the ambient secondary organic aerosol size distribution, *Atmospheric Environment*, 27, 2403 – 2416, 1993.

Paspastefanou, C.: Residence time of tropospheric aerosols in association with radioactive nuclides, *Applied Radiation and Isotopes*, 64, 93 – 100, 2006.

245 Wexler, A. and Seinfeld, J.: The distribution of ammonium salts among a size and composition dispersed aerosol, *Atmospheric Environment*, 24A, 1231 – 1246, 1990.

Zhang, X., Pandis, S., and Seinfeld, J.: Diffusion-limited versus quasi-equilibrium aerosol growth, *Aerosol Science and Technology*, 46, 874 – 885, 2012.